Gas Tunnel Type Plasma Spraying of Silicon Carbide Films for Thermoelectric Applications†

FAHIM F. Narges and KOBAYASHI Akira

Abstract

Silicon carbide deposition is an attractive process for aerospace applications requiring properties of chemical and mechanical resistance at ultra-high temperatures. The main objective of the research is the fabrication and characterization of plasma sprayed deposition of silicon carbide films for high temperature thermoelectric applications. Gas tunnel plasma spraying has been applied successfully for the deposition of SiC films on stainless steel substrates.The microstructure and surface morphology of the SiC films were characterized by means of X-ray diffraction (XRD) and scanning electron microscope (SEM). The control of the processing parameters such as powder feeding rate, composition of plasma working gases, spraying distance, and carrier gas flow rate allowed the deposition of dense, uniform, continuous, and high purity crystalline SiC films. The thickness of the SiC films varied from 3 μm to 10 μm.

KEYWORDS: (Silicon carbide), (Gas tunnel plasma spraying), (Thermoelectric materials), (Microstructure).

1. Introduction

Silicon carbide is a promising candidate for high temperature and high power applications such as the nose and leading edges of re-entry space vehicles because of their high thermoelectric power, high thermal stability, high resistance to oxidation and corrosion, their nontoxicity, and excellent mechanical properties. Thus, SiC is expected to be used as a thermoelectric material at high temperatures[1, 2]. Deposition of SiC films and coatings with conventional deposition techniques such as thermal chemical vapor deposition (CVD), plasma enhanced CVD, sputtering, and laser-assisted methods have difficulty in satisfying the requirements of industrial applications because these processes are comparatively time consuming for the deposition of thick coatings due to their low deposition rate (generally < 1 nm/s). In addition, the necessity to use hazardous source gases and/or the generation of corrosive by-products is a common disadvantage of conventional techniques. Therefore, it is of great interest to develop a novel method that can overcome these drawbacks.

Gas tunnel type plasma jet is one of the most important technologies for synthesizing functional materials, because the plasma jet has high temperature and high heat capacity under various operating conditions. Also, it operates at a high voltage and with easy control of power. The thermal efficiency of the gas tunnel plasma jet is about 80 %, which is much higher than that of conventional types of plasma jet (≈ 50 %). Thus, it is possible to achieve the production of ultrafine particles and spray coatings of refractory materials[3-6].

In this study, the deposition of SiC films on stainless-steel substrates using SiC powder as a starting material was investigated with the gas tunnel type plasma spraying technique. The microstructure and surface morphology of the SiC films were mainly examined.

2. Experimental

2.1. Preparation of SiC films

High Purity (> 97 %) 2H-SiC powder of particle size 20-45 μm was atmospherically plasma sprayed (APS) on flat 304 stainless-steel substrates by using the gas tunnel type plasma jet (**Fig. 1**). The substrates of dimension 50 x 50 x 2 mm were grit-blasted with alumina grit on one side to clean and roughen the surface and followed by ultrasonic cleaning using acetone to remove any greases and other contamination.

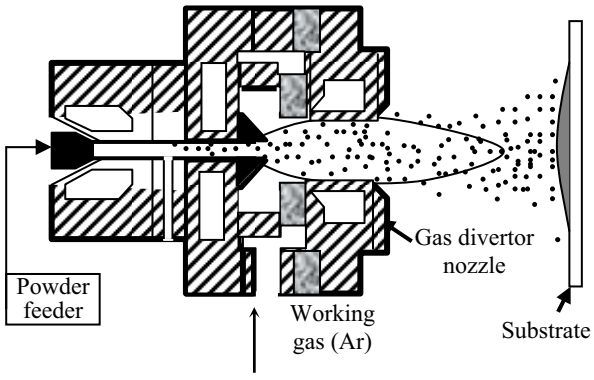

Fig. 1. Systematic diagram of gas tunnel type plasma spraying torch and experimental set up.

† Received on November 7, 2005
* Foreign Visiting Researcher
** Associate Professor

Transactions of JWRI is published by Joining and Welding Research Institute, Osaka University, Ibaraki, Osaka 567-0047, Japan

Table 1 The processing parameters.

DC plasma current (A)	400,450,500
Primary gas flow rate (Ar, l/min)	120-150
Secondary gas flow rate (N_2, l/min)	10-15
Carrier gas (Ar, l/min)	7,9,11,14
Powder feed rate (g/min)	5
Spray distance (mm)	35,40,45
Spray time (sec)	20,40

SiC powders were internally fed inside the plasma flame stream to meet maximum temperature because SiC has a high melting point ≈ 2700°C. The deposition was performed under the spraying parameters listed in **Table 1**. Argon and nitrogen gases were used as the plasma gas.

2.2. Characterization techniques

The surface morphology of the feedstock and SiC films cross-sections was examined by ERA8800FE scanning electron microscope. The examined cross-section samples were mounted in epoxy resin using a HMP-Molding hand press, Wingo Seiki Co., Ltd. Osaka, Japan, polished by using a Buehler Metaser V Grinder-polisher and buffed with alumina paste (1.0, 0.3, and 0.05 μm, respectively) to get a mirror finished surface. All examined samples were coated with a thin film of gold using gold ion sputtering system (Thermo VG Scientific Polaron Sc7620 Sputter Coater) to make them electrically conductive before SEM observation.

Phase constituents of feedstock powder and SiC deposits were identified by using a JEOL JDX-3530M X-ray diffractometer system with CuKα radiation source at a voltage of 40 kV and current of 40 mA.

3. Results and Discussion

3.1. Microstructure of feedstock powder

Figure 2 shows the SEM images of the SiC feedstock. It is clear from the SEM micrographs that the particle size of the powder ranged from 20 to 45 μm. Also, we can notice that the crystal structure is hexagonal.

The XRD pattern of typical feedstock powder is depicted in **Fig. 3**. The peaks corresponding to α- SiC (100), (101), (103), (200), (201), and (112) planes were clearly presented. Moreover, the (002), (110), and (004) peaks due to the presence of β- SiC have been detected.

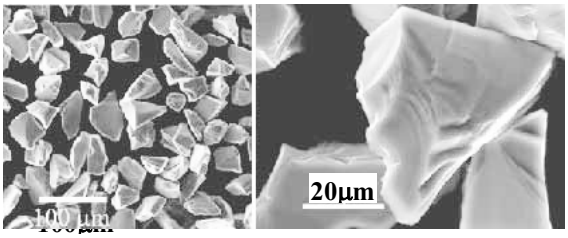

Fig.2. SEM micrographs of SiC feedstock powder.

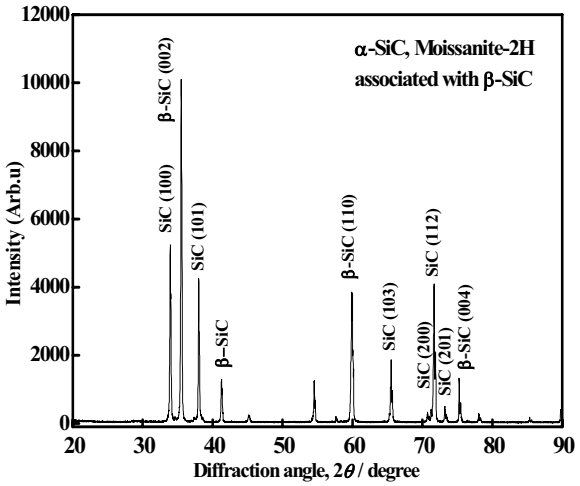

Fig. 3 XRD pattern of SiC feedstock powder.

3.2. Microstructure of plasma-sprayed SiC films

3.2.1. Different Ar carrier flow rate

Figure 4 shows the XRD patterns of plasma-sprayed SiC films deposited at different Ar carrier gas flow rates of (a) 4 l/min, (b) 7 l/min and (c) 11 l/min, plasma current: I = 450 A, primary plasma gas (Ar) flow rate: Q = 120 l/min, spraying distance: L = 45 mm, and spraying time: t = 40 sec. The XRD patterns revealed that the peaks corresponding to α and β- SiC films. Also, other peaks were detected corresponded to stainless-steel substrate because the thickness of these films is around 3 μm as shown in **Fig. 5**.

SEM of the cross-section of the film sprayed at: plasma current: 450 A, Ar flow rate: 4 l/min, Ar plasma gas flow rate: 120 l/min, spraying distance: 45 mm, and spraying time: 40 sec are shown in Fig. 5. It was revealed that the SiC deposit was compact, smooth, dense, free from pores, adhering well, and showed no cracking. The absence of pores in the SiC deposit indicated that the SiC particles did not resolve to decompose during deposition.

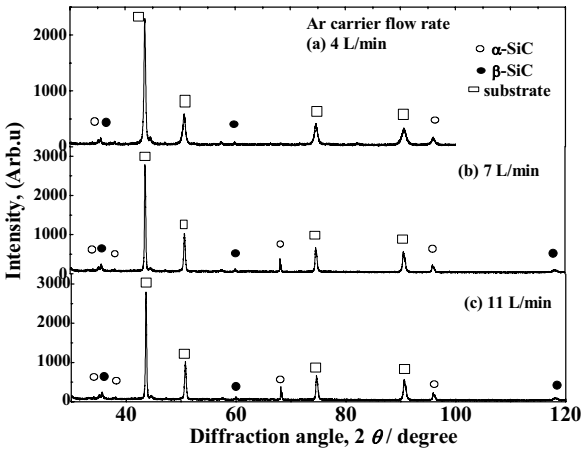

Fig.4. XRD patterns of SiC films on stainless-steel substrate sprayed at different Ar carrier gas flow rate (a) 4 l/min, (b) 7 l/min and (c) 11 l/min.

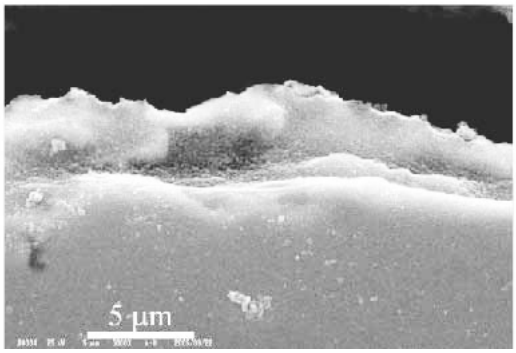

Fig.5. SEM of the cross-section of the film sprayed at: plasma current: 450 A, Ar flow rate: 4 l/min, Ar plasma gas flow rate: 120 l/min, spraying distance: 45 mm, and spraying time: 40 sec.

3.2.2. Plasma composition gas

Figure 6 shows the XRD patterns of SiC films sprayed under different compositions of plasma gas (a) primary plasma gas 150 Ar l/min and (b) primary plasma gas (Ar): 120 l/min; and secondary plasma gas (N_2): 15 l/min. Clearly, the XRD peaks corresponding to α and β-SiC films become more sharp and intense. The intensity of substrate peaks was decreased compared with previous conditions because the thickness of SiC films was increased to about 10 μm as shown in **Fig. 7**. There are no peaks due to Si or SiO_2 detected in the XRD spectra in contrast to that reported by Kang [7]. He noted that when SiC feedstock powder was injected into the plasma jet, SiC particles in the plasma temperature region heated and simultaneously decomposed as follows:

$$SiC_{(s)} + 3/2\ O_{2\ (g)} \rightarrow SiO_{2(s)} + CO_{(g)} \quad ---(1)$$

$$SiC_{(s)} + O_{2\ (g)} \rightarrow Si_{(s,l)} + CO_{2(g)} \quad -----(2)$$

$$SiC_{(s)} + 1/2O_{2\ (g)} \rightarrow Si_{(s,l)} + CO_{(g)} \quad ----(3)$$

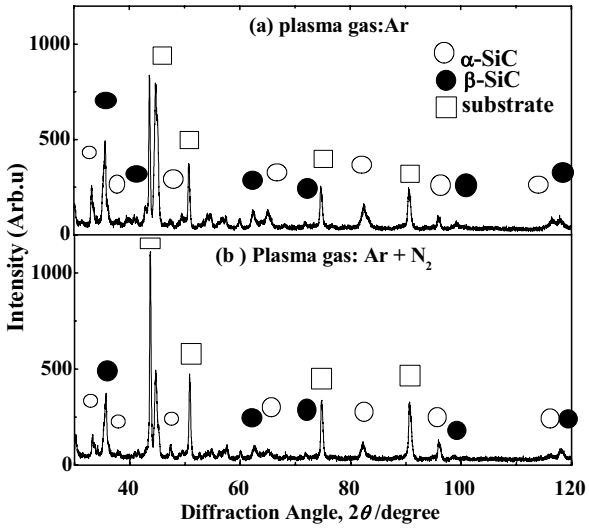

Fig. 6. XRD patterns of SiC films deposited at different composition of plasma gas (a) Ar 150 l/min and (b) 120 Ar l/min + 15 N_2 l/min.

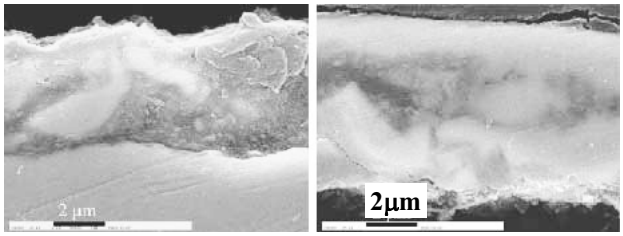

Fig.7. SEM images of the cross-section of the SiC films sprayed at primary gas flow rate: 120 Ar l/min, secondary gas flow rate: 15 N_2 l/min, plasma current: 400 A, carrier flow rate: 14 l/min, spraying distance: 45 mm, and spraying time: 20 sec

Figure 7 shows the SEM images of the cross-section of the SiC films sprayed at primary gas flow rate: 120 Ar l/min, secondary gas flow rate (N_2): 15 l/min, plasma current: 400 A, carrier flow rate: 14 l/min、spray distance: 45 mm, and spray time: 20 sec. The SEM results indicated that the sprayed SiC films were uniform, continuous, and highly pure. Also, the sprayed SiC films are free from pores (due to escaping of CO or CO_2 gases during decomposition).

4. Conclusions

The following conclusions can be drawn from the present study:

(1) X-ray study confirmed the presence of α and β-SiC phases in the sprayed films and decomposition of SiC was not confirmed after the deposition.
(2) SEM studies revealed that the sprayed SiC formed on the surface of stainless-steel substrate has a compact, smooth, and dense morphology.
(3) The thickness of the sprayed SiC deposits varied from nearly 3 μm to 10 μm depending on the spraying parameters.

Thermoelectrical characterization and increasing the thickness of sprayed SiC films will be the subjects of future research.

References

1) J.S. Pelt, M. E. Ramsey, S. M. Durbin, Thin Solid Films **371** (2000) 72-79.
2) Y. Sun, T. Miyasato, J. K. Wigmore, N. Sonoda, Y. Watari, J. Appl. Phys. **82** (1997) 2334-2340.
3) Y. Arata, A. Kobayashi, Y. Habara, J. Appl. Phys. **62** (5) (1987) 4884-4889.
4) A. Kobayashi, Weld. International, **4** (4) (1990) 276-282.
5) Y. Arata, A. Kobayashi, and Y. Habara, J. High. Tem. Soc.**18** (2) (1992) 25-32.
6) Y. Arata and A. Kobayashi, J. Appl. Phys., **59** (No. 9) (1986) 3038-3044.
7) H. K. Kang, Scripta Materialia **51** (2004) 1051- 1055.